

Measurements of Fe and Ar Fragmentation Cross Sections

K. H. Lau, R. A. Mewaldt, and E. C. Stone
California Institute of Technology
Pasadena, California 91125 USA

Measurements are reported of the yields of individual isotopes of Cr to Co ($Z = 24$ to 27) resulting from the fragmentation of ^{56}Fe , and the isotopes of Mg to K ($Z = 12$ to 19) resulting from the fragmentation of ^{40}Ar .

1. Introduction - Recent advances in the resolution and collecting power of cosmic ray instrumentation, have led to dramatic improvements in the precision of cosmic ray composition measurements, both elemental and isotopic. The interpretation of these measurements is presently limited by uncertainties in the fragmentation cross-sections needed to correct for nuclear interactions with the interstellar gas. Cosmic ray propagation codes now rely mainly on semi-empirical cross-section formulae developed by Silberberg and Tsao (S&T), which have a typical uncertainty of $\sim 25\%$ [1].

We report here relative isotope yields from the fragmentation of ~ 380 MeV/nucleon ^{56}Fe and ~ 210 MeV/nucleon ^{40}Ar in CH_2 targets, observed during the calibration of two cosmic ray spectrometers at the Lawrence Berkeley Laboratory Bevalac, and compare these with calculated yields based on the S&T cross-section formulae [1]. Preliminary results from the ^{40}Ar study were reported by Lau, Mewaldt, and Wiedenbeck (LMW) [2].

2. Experimental Setup - The experimental data were obtained during Bevalac runs in April, 1978 (^{56}Fe) and April, 1981 (^{40}Ar). A description of the experimental setup for the ^{40}Ar calibration is given in reference [2]; with additional details in [3]. The setup for the ^{56}Fe run was essentially identical except that the fragmentation products were measured during the calibration of the Caltech Heavy Ion Spectrometer Telescope (HIST) [4], launched on ISEE-3. In the ^{56}Fe run a 587 MeV/nucleon beam was incident on a 5.28 g/cm^2 thick CH_2 target, such that the energy of the interactions ranged from ~ 100 to 580 MeV/nucleon, with a mean interaction energy of ~ 380 MeV/nucleon. In the ^{40}Ar runs the beam energy was 287 MeV/nucleon, the CH_2 target thickness 4.1 g/cm^2 , and the interaction energy ranged from ~ 70 to 280 MeV/nucleon with a mean of ~ 210 MeV/nucleon. We estimate that $\sim 70\%$ (90%) of the analysed interactions occurred in the CH_2 target for the Fe (Ar) runs, the balance taking place in other material including Al and air.

As discussed in LMW, because the experimental setup was designed for calibration purposes, absolute cross-sections could not be measured. In particular, the detectors intercepted only those fragments emitted within $\sim 1^\circ$ of the beam direction. On the other hand, with the excellent mass resolution achieved, *relative* fragmentation yields can be determined, which are adequate for many cosmic-ray studies (see, e.g., [5]).

3. Data Analysis - For the ^{56}Fe data we use the isotope identification techniques developed for HIST flight data (see, e.g., [6]), where we have restricted the analysis to events stopping in the last four detectors. Figure 1 shows examples of the observed mass distributions, along with Gaussian fits to the data. The excellent mass resolution ($\sigma_m \approx 0.25 \text{ amu}$) permits the isotopes ^{53}Fe , ^{54}Fe , and ^{56}Fe to be resolved in the presence of (much more abundant) ^{56}Fe . The relative isotope fractions that we observe for Cr, Mn, and Fe fragments are given in Table 1.

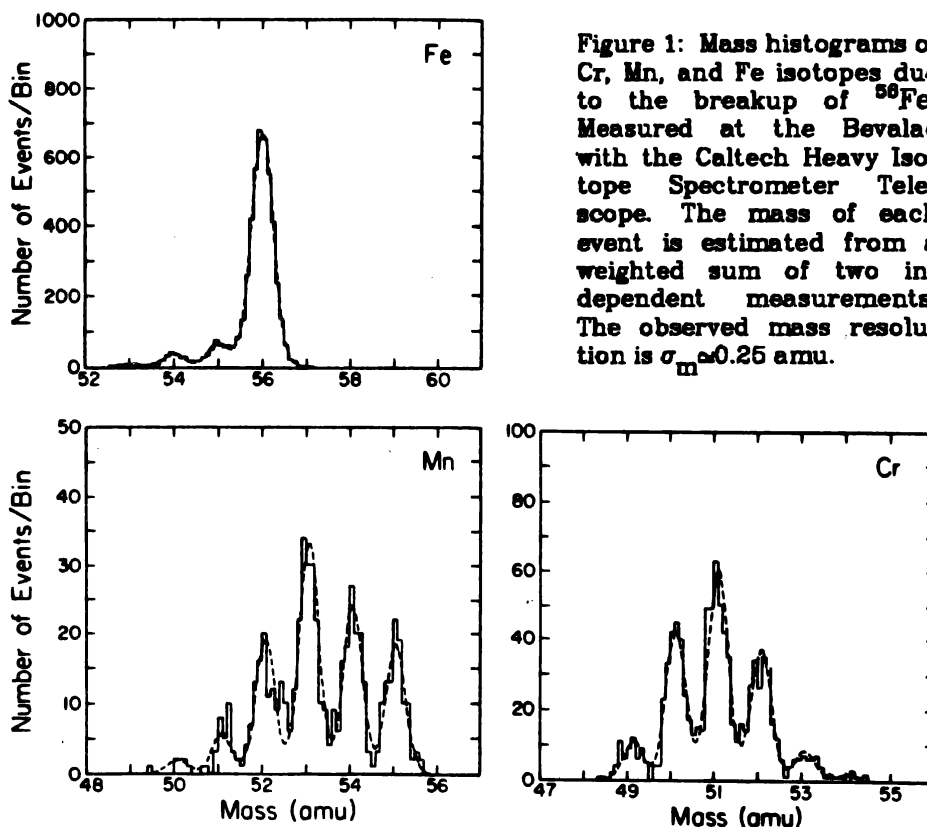


Figure 1: Mass histograms of Cr, Mn, and Fe isotopes due to the breakup of ^{56}Fe . Measured at the Bevalac with the Caltech Heavy Isotope Spectrometer Telescope. The mass of each event is estimated from a weighted sum of two independent measurements. The observed mass resolution is $\sigma_m \approx 0.25$ amu.

The analysis of the ^{40}Ar data set has already been described [2,3]. Table 2 summarizes the fractional yield of isotopes (within each element) for Mg to K fragments ($12 \leq Z \leq 19$). The $14 \leq Z \leq 18$ data are essentially the same as those in [2] (with minor differences due to improved statistics and refined corrections), but they are presented in this form for the first time. The Mg and Al data have not been presented before. We find excellent agreement between our isotope fractions and those reported by Viyogi et al. [7], who analyzed the fragmentation of ^{40}Ar in a C target at 213 MeV/nucleon. This suggests that the relative isotope yields do not depend strongly on the target material. Comparing our isotope fractions (Table 2) with those of Viyogi et al. we find no evidence for a mass-dependent bias within an element such as might be introduced by our limited angular coverage.

4. Comparison with Calculated Fragmentation Yields - As described in LMW we have used a Monte Carlo approach developed by M.E. Wiedenbeck to model the experimental setup and calculate the expected yield of each isotope. The calculation takes into account both the energy and target

Isotope	Fraction of Element	
	Observed	Calculated
^{56}Fe	0.669 ± 0.010	0.496 ± 0.003
^{54}Fe	0.273 ± 0.009	0.268 ± 0.002
^{53}Fe	0.058 ± 0.005	0.236 ± 0.002
^{56}Mn	0.215 ± 0.007	0.250 ± 0.002
^{54}Mn	0.286 ± 0.008	0.356 ± 0.003
^{53}Mn	0.305 ± 0.008	0.220 ± 0.002
^{52}Mn	0.146 ± 0.008	0.126 ± 0.002
^{51}Mn	0.038 ± 0.003	0.040 ± 0.001
^{50}Mn	0.010 ± 0.002	0.008 ± 0.001
^{54}Cr	0.026 ± 0.003	0.023 ± 0.001
^{53}Cr	0.088 ± 0.005	0.129 ± 0.002
^{52}Cr	0.294 ± 0.009	0.375 ± 0.002
^{51}Cr	0.315 ± 0.009	0.280 ± 0.002
^{50}Cr	0.219 ± 0.008	0.157 ± 0.002
^{49}Cr	0.058 ± 0.004	0.036 ± 0.001

dependence of the cross-sections [8] for the various materials traversed. Tables 1 and 2 include the calculated isotope fractions for comparison with the observations.

Figure 2 shows a comparison of the measured and calculated isotope yields from ^{56}Fe (normalized to the sum of Cr and Mn). While there is general agreement on the shape of the distributions, there are also significant differences. For example, the calculation predicts $\text{Mn}/\text{Cr}=0.82$, while we find $\text{Mn}/\text{Cr}=1.23\pm 0.04$, a discrepancy also noted by others [9,10,11] who measured at a variety of energies with C, CH_2 , and H targets. Of related astrophysical interest is the result that the radioactive isotope ^{54}Mn fraction is lower than calculated.

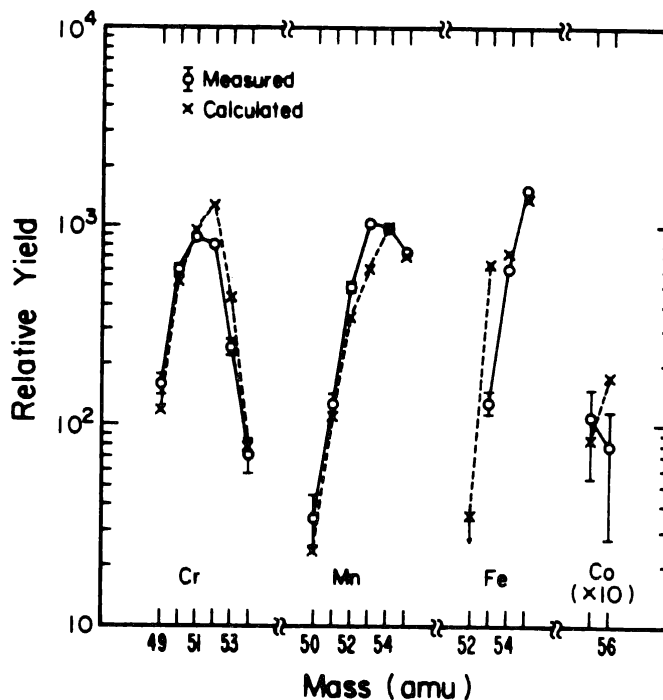


Figure 2: A comparison of measured and calculated yields, normalized to the sum of Mn and Cr.

Table 2 - ^{40}Ar Fragmentation		
Isotope	Fraction of Element	
	Observed	Calculated
^{40}K	0.415 ± 0.080	0.392 ± 0.026
^{39}K	0.585 ± 0.080	0.409 ± 0.026
^{38}K	<0.03	0.199 ± 0.021
^{36}Ar	0.509 ± 0.017	0.477 ± 0.006
^{38}Ar	0.324 ± 0.016	0.357 ± 0.006
^{37}Ar	0.125 ± 0.011	0.143 ± 0.004
^{36}Ar	0.042 ± 0.007	0.023 ± 0.002
^{39}Cl	0.169 ± 0.013	0.130 ± 0.004
^{38}Cl	0.146 ± 0.012	0.217 ± 0.005
^{37}Cl	0.296 ± 0.015	0.248 ± 0.005
^{36}Cl	0.253 ± 0.015	0.273 ± 0.005
^{35}Cl	0.115 ± 0.011	0.112 ± 0.004
^{34}Cl	0.021 ± 0.005	0.020 ± 0.002
^{38}S	0.009 ± 0.003	0.003 ± 0.000
^{37}S	0.042 ± 0.006	0.027 ± 0.001
^{36}S	0.126 ± 0.010	0.150 ± 0.001
^{35}S	0.218 ± 0.012	0.274 ± 0.001
^{34}S	0.358 ± 0.014	0.377 ± 0.002
^{33}S	0.189 ± 0.012	0.130 ± 0.001
^{32}S	0.057 ± 0.007	0.039 ± 0.001

Table 2 (continued)		
Isotope	Fraction of Element	
	Observed	Calculated
^{36}P	0.027 ± 0.006	0.019 ± 0.001
^{34}P	0.088 ± 0.011	0.088 ± 0.001
^{33}P	0.241 ± 0.017	0.300 ± 0.002
^{32}P	0.341 ± 0.019	0.328 ± 0.002
^{31}P	0.253 ± 0.017	0.211 ± 0.002
^{30}P	0.050 ± 0.009	0.054 ± 0.001
^{32}Si	0.052 ± 0.010	0.088 ± 0.001
^{31}Si	0.137 ± 0.015	0.203 ± 0.002
^{30}Si	0.387 ± 0.022	0.408 ± 0.002
^{29}Si	0.294 ± 0.020	0.206 ± 0.002
^{28}Si	0.130 ± 0.015	0.095 ± 0.001
^{30}Al	0.040 ± 0.013	0.052 ± 0.001
^{29}Al	0.158 ± 0.024	0.225 ± 0.003
^{28}Al	0.275 ± 0.029	0.313 ± 0.003
^{27}Al	0.410 ± 0.032	0.303 ± 0.003
^{26}Al	0.117 ± 0.021	0.107 ± 0.002
^{27}Mg	0.094 ± 0.024	0.145 ± 0.002
^{26}Mg	0.306 ± 0.038	0.388 ± 0.003
^{25}Mg	0.406 ± 0.041	0.285 ± 0.003
^{24}Mg	0.194 ± 0.033	0.182 ± 0.003

The two largest discrepancies in either data set are at ^{53}Fe and ^{38}K , both of which are ~ 6 times less abundant (fraction of element) than calculated. Since both nuclei have 1 less neutron than a "magic number" ($n=20-1$ for ^{38}K , $n=28-1$ for ^{53}Fe), their yield may be suppressed if neutron emission is involved. The S&T formulas do not take nuclear shell-structure into account except for a "pairing" correction. Although there are other nuclei with $n=19$ or $n=27$ that do not exhibit such a dramatic effect, we suggest that nuclear shell structure should be examined carefully in any attempts to improve semi-empirical cross-sections.

Other significant discrepancies between the observed and calculated fractional yields (e.g., ^{37}Cl , ^{38}Cl , ^{39}Cl , and ^{36}S) involve peripheral reactions, which S&T calculate with special formulae. The agreement for such reactions is better for ^{56}Fe , but these reactions should be less important at the higher energies appropriate to the ^{56}Fe data set.

For both ^{56}Fe and ^{40}Ar fragments the medians of the observed mass distributions are lower than calculated (Figure 2 above and Figure 3 in [2]). There are also differences in the widths of the distributions that are less easily characterized. For both data sets, the ratio of the calculated to measured isotope fractions exhibit rms differences of 25%. Although consistent with the claimed accuracy of the S&T formulae, this demonstrates the need for further cross section measurements if the potential of cosmic ray composition measurements is to be realized.

Acknowledgements: We are grateful to Dr. M. E. Wiedenbeck, who developed the Monte Carlo approach for evaluating the semi-empirical cross-section formulae, for helpful discussions on a number of aspects of this work. Dr. J. D. Spalding was responsible for developing most of the techniques for resolving Fe isotopes in HIST and offered advice on several occasions. We also thank Dr. H. C. Crawford for help with the Bevalac calibrations. This work was supported in part by NASA under grant NGR 05-002-160 and contract NAS5-28449.

References

1. R. Silberberg and C. H. Tsao, *Ap.J. Suppl.*, 25, 315, 1973, and 25, 335, 1973; C.H. Tsao and R. Silberberg, *Proc. 16th Int. Cosmic Ray Conf.* 2, 202, 1979; R. Silberberg, C.H. Tsao, and John R. Letaw, *Composition and Origin of Cosmic Rays*, ed. M.M. Shapiro, Reidel, p. 321, 1983, and references therein.
2. K.H. Lau, R.A. Mewaldt and M.E. Wiedenbeck, *Proc. 18th Int. Cosmic Ray Conf.* 9, 255, 1983.
3. K.H. Lau *Ph.D. Thesis, Caltech, 1985*
4. W.E. Althouse et al., *Geosci. Electronics, GE-16*, 204, 1978.
5. E.C. Stone and M.E. Wiedenbeck *Ap.J.*, 231, 95, 1979.
6. R.A. Mewaldt, J.D. Spalding, E.C. Stone and R.E. Vogt, *Ap. J.* 235, L95, 1980.
7. Y.P. Viyogi, et al., *Physical Review Letters* 42, 33, 1978.
8. R. Silberberg and C.H. Tsao, *Proc. 15th Int. Cosmic Ray Conf.*, 2, 89, 1977.
9. G.D. Westfall, et al., *Physical Review C*, 19, 1309, 1979.
10. M. Poferl-Kertzman, P.S. Freier and C.J. Waddington, *Proc. 17th Int. Cosmic Ray Conf.* 9, 187, 1981.
11. W.R. Webber and D. Brautigam, *Ap.J.* 260, 894, 1982.